

Evaluation of Multispectral Data for Rapid Assessment of Wheat Straw Residue Cover

D. G. Sullivan,* J. N. Shaw, P. L. Mask, D. Rickman, E. A. Guertal, J. Luvall, and J. M. Wersinger

ABSTRACT

Crop residues influence near surface soil organic carbon (SOC) content, impact our ability to remotely assess soil properties, and play a role in global carbon budgets. Methods that measure crop residues are laborious, and largely inappropriate for field-scale to regional estimates. The objective of this study was to evaluate high spectral resolution remote sensing (RS) data for rapid quantification of residue cover. In March 2000 and April 2001, residue plots (15 by 15 m) were established in the Coastal Plain and Appalachian Plateau physiographic regions of Alabama. Treatments consisted of five wheat (*Triticum aestivum* L.) straw cover rates (0, 10, 20, 50, and 80%) replicated three times. Spectral measurements were acquired monthly via a handheld spectroradiometer (350–1050 nm) and per availability via the Airborne Terrestrial Applications Sensor (ATLAS) (400–12 500 nm). Overall, treatment separation was influenced by soil water content and percentage of total organic carbon (TOC) of the residue (degree of decomposition). Results showed that atmospherically corrected visible and near-infrared ATLAS data can differentiate between residue coverages. Similar results were obtained with the handheld spectroradiometer, although treatment differentiation was less consistent. Thermal infrared ATLAS imagery best discriminated among residue treatments due to differing heat capacities between soil and residue. Results from our study suggest airborne thermal infrared (TIR) imagery can be used for crop residue variability assessment within the southeastern USA.

ADOPTION OF MINIMUM tillage with residue management strategies has been widely associated with improvements to soil quality. Crop residue management enhances soil quality primarily through the accumulation of SOC. Benefits attributable to residue management include reduced erosion, improved infiltration, and soil aggregation (Prasad and Power, 1991). Since 33% of agricultural lands in the USA have been classified as highly erodible, residue management can effectively reduce erosion and off-site transport of nutrients and pesticides (USDA, 1995; McMurtrey et al., 1993; Lal and Kimble, 1997). A rapid method of monitoring field-scale distribution of residue cover could help better establish the benefits of conservation tillage to soil and water quality.

Problems with field-scale residue coverage assessments arise because obtaining spatially representative estimates of residue cover in a timely and cost efficient manner is difficult. Cover estimates are increasingly important due to eligibility and compliance with government cost-

share programs, such as the Environmental Quality Incentives Program (EQIP). According to the 1985 Food Security Act, lands considered 'highly erodible' must implement an acceptable conservation program to remain eligible for farm benefits. Furthermore, cost-share recipients for reduced tillage systems must maintain a minimum of 30 to 50% crop residue cover to receive program reimbursements. Current line-transect techniques are labor intensive and accuracy is often a function of line length and the number of data points collected. Remote sensing techniques using high spatial and spectral resolution sensors may facilitate field-scale and regional crop residue cover assessment.

Unlike growing vegetation, there is a general lack of information regarding spectral signatures associated with decaying crop residues. However, a fundamental understanding of molecular functional groups in growing and senescent vegetation provides a foundation for addressing residue spectra. Functional groups present in plant material, such as CH₃, OH, and H₂O, significantly affect spectral response properties via the presence of absorption bands within the 700- to 2600-nm range (Murray and Williams, 1988). During the initial stages of tissue chlorophyll loss, spectral response is greatest from 400 to 800 nm, as senescent plant tissues absorb incoming blue (300–400 nm) and red (500–600 nm) spectra while reflecting green (400–500 nm). Presence of water at this stage masks absorbance features in the near infrared (NIR) associated with lignin and cellulose (Elvidge, 1990). As decay progresses, the relative abundance of lignin and cellulose present is evidenced by broad absorption bands throughout the 400- to 900-nm spectral region (Elvidge, 1990).

Studies conflict regarding the use of remote sensing data to reliably differentiate between residue and soil. Early attempts to differentiate between soil and residue spectra showed differences in spectral reflectance were greatest in the NIR (Gausman et al., 1973; Aase and Tanaka, 1991). These results are in congruence with a similar study conducted by McMurtrey et al. (1993). McMurtrey et al. (1993) developed a vegetation index using spectrophotometer data of five different crop residues and four different soil types. McMurtrey et al. (1993) found reflection at 450, 660, and 830 nm captured most differences between soil and crop residue spectra in a laboratory setting. In another study, Daughtry et al. (1995) utilized reflectance data to distinguish between a variety of crop residues and soils representing 14 sub-orders. Results showed visible (VIS) and NIR energy could not reliably distinguish soil from residue due to variability in soil properties, water content, and residue

D.G. Sullivan, USDA-ARS Southeast Watershed Research Laboratory, Tifton, GA 31794; J.N. Shaw, P.L. Mask, and E.A. Guertal, Dep. of Agronomy and Soils, Auburn University, Auburn, AL 36849; D. Rickman and J. Luvall, Global Hydrology and Climate Center, Huntsville, AL 35805; J.M. Wersinger, Physics Dep., Auburn University Auburn, AL 36849. Received 25 May 2004. *Corresponding author (dgs@tifton.usda.gov).

Published in Soil Sci. Soc. Am. J. 68:2007–2013 (2004).
© Soil Science Society of America
677 S. Segoe Rd., Madison, WI 53711 USA

Abbreviations: ATLAS, Airborne Terrestrial Applications Sensor; CAI, cellulose absorption index; CV, coefficient of variation; NIR, near infrared; RS, remote sensing; SOC, Soil organic carbon; TC, total carbon; TIR, thermal infrared; TOC, total organic carbon; VIS, visible.

age. Nagler et al. (2000) applied the cellulose absorption index (CAI) developed by Daughtry et al. (1996) to differentiate among residue samples arranged on a black 45 by 45 by 2.5 cm plate using a controlled illumination source. As residue decomposed, CAI values decreased. Findings were confounded by water, litter type, and decomposition stage. More recently, Daughtry (2001) used the CAI to differentiate between spectral response patterns of corn (*Zea mays* L.), soybean (*Glycine max* L.), and wheat residue and five soil types at different soil water contents. Samples were arranged in 45-cm square trays consisting of soil or residue, mixed scenes of soil and residue were then simulated. Daughtry (2001) was able to discern the relative amount of residue present, via a positive CAI value. Although moist conditions yielded lower CAI values for residue, the CAI for soil remained constant.

Laboratory and field studies have had some success differentiating among residue coverages based on spectral response patterns. Under controlled laboratory conditions, properly calibrated red and NIR spectra may differentiate among degrees of residue cover. Thermal infrared spectra also show promise as a new method for assessing field scale variability in crop residue coverage. However, due to the expense associated with high-resolution TIR imagery, little has been done to investigate TIR as an alternate method of crop residue assessment. Rapid assessment of residue cover is particularly important in the southeastern USA where residue management may significantly impact soil quality and sustainability of these highly weathered soil systems. Thus, the goals of this study are two-fold: (i) evaluate handheld radiometer data and atmospherically corrected airborne imagery as a means to assess ground cover at a large plot scale, and (ii) evaluate high spectral resolution TIR spectra as a method for depicting crop residue coverage at a large plot scale.

MATERIALS AND METHODS

Study Sites

Study sites were located in two physiographic provinces of Alabama. The Coastal Plain study site was located in Headland, AL, at the Alabama Agricultural Experiment Station (AAES) Wiregrass Research and Extension Center (85°19'03" W, 31°21'56" N). Soils formed in sandy and loamy fluvial-marine sediments and classify predominantly as fine-loamy, kaolinitic, thermic Plinthic and Typic Kandudults. Epipedons in this region were predominantly loamy sand texture. This region is intensively cropped to peanuts (*Arachis hypogaea*), cotton (*Gossypium hirsutum* L.), and corn. The second study site was located in the Appalachian Plateau near Crossville, at the

Sand Mountain AAES Research and Extension Center (85°57'39" W, 34°16'41" N). Soils classify as fine-loamy, siltaceous, subactive, thermic Typic Hapludults. Soils formed from acid sandstone residuum and typical epipedons have a sandy loam/loam texture. Most of the sampling area is typically cropped to corn.

Wheat straw residue applications were designed to mimic a conventional double-cropped system (wheat–cotton or wheat–soybean) to evaluate residue spectra during periods of minimal warm season crop cover. Plots (15 by 15 m) were established on weed-free, fresh-tilled surfaces in March 2000 and repeated in April 2001. Pre- and postemergent herbicides were used to control weeds and grasses. Residue cover was calculated on a mass basis as a percentage of the amount of residue necessary for complete ground cover. Treatments consisted of five residue cover rates (0, 10, 20, 50, and 80%) arranged in a completely randomized design. A digital camera was used to acquire images of each plot at inception and classified in 2000 to ensure treatment coverages were met. Monthly digital images were taken in 2001 to monitor changes in residue cover over the year, and average estimates of cover per treatment were used in regression analyses

Laboratory

Composite soil samples were collected within each plot at the onset of the study (0–1 cm) before residue application to determine near-surface soil properties. Soils were air-dried and sieved to pass a 2-mm sieve. Analyses included total C via dry combustion on pulverized samples, citrate-dithionite extractable Fe (Jackson, 1975), and particle-size distribution on the <2-mm fraction (Kilmer and Alexander, 1949). Near surface soil attributes were similar across sites differing primarily by silt and sand content, with Appalachian Plateau soils having greater silt content and lesser amounts of sand (Table 1). Near-surface samples (0–1 cm) coincident with each remotely sensed data acquisition were also collected for gravimetric water content (θ_g).

Surface residues were sampled monthly, weighed, dried, and reweighed for water content. A separate sample was collected for C content as a means to assess residue decomposition. Samples for C content were collected bimonthly via fistula bags (10 × 20 cm), which were filled with straw and staked within each plot at the onset of the study. Wheat straw was dried and roll ground for total C content via dry combustion of a 0.06- to 0.16-g sample using a LECO CHN-600 analyzer (Leco Corp., St. Joseph, MI).

Sensors

GER 1500 Spectroradiometer

Reflectance measurements were collected monthly April through June and October through December, on clear days using a hand-held GER 1500 spectroradiometer (GER Corp., New York). The GER 1500 uses a diffraction grating of silicon photo diodes with 512 individual detectors, and collects data

Table 1. Mean and standard deviations of near-surface soil properties (0–1 cm) observed at the Appalachian Plateau and Coastal Plain study sites.

Site	Soil property				
	Sand	Silt	Clay	SOC	Fe _d ‡
	%				
Appalachian Plateau	55.5 (1.20)†	37.8 (1.13)	6.7 (1.14)	0.57 (0.03)	0.21 (0.01)
Coastal Plain	79.6 (0.92)	12.6 (0.44)	7.9 (0.73)	0.53 (0.02)	0.25 (0.02)

† Standard deviations are given in parentheses.

‡ Citrate-dithionite extractable Fe.

between 350 to 1050 nm in 1.5-nm increments. Wavelengths utilized in this study encompassed the 520- to 900-nm spectrum to coincide with the spectral band passes of the ATLAS. Plot data were collected as close to solar noon as possible under clear conditions. Measurements were taken at nadir, within an 8° field of view, from a distance of 2.4 m above ground to approximate a spatial resolution of 0.30 m². Data collection consisted of five measurements from within each plot. Measurements were converted to percent reflectance based on the reflectance properties of a spectralon reference plate. The spectralon reflectance plate was placed horizontally on the ground outside of each plot. Reference data were collected from a distance of approximately 25 cm from the spectralon plate.

Airborne Terrestrial Applications Sensor (ATLAS)

The ATLAS multispectral scanner acquired data onboard a Lear jet flown at approximately 1400 m. Airborne Terrestrial Applications Sensor collects data in 15 nominal bands ranging from 400 to 12 500 nm, with an approximate spatial resolution of 2.5 m at nadir, and a 72° field of view (Birk, 1992) (Table 2). Simultaneous with acquisition the system records 6° of geometric data: latitude, longitude, pitch, roll, altitude, and heading. The onboard radiometric calibration subsystem consisted of three active sources: integrating sphere, hot black body, and cold black body. These are referenced on each revolution of the scan mirror. Data from the active calibration sources within the sensor were used to develop a system transfer function on a per scan line basis. The specific technique used accounts for sensor drift while eliminating high frequency noise. The result of this process converts each of the original airborne measurements recorded in eight bits per pixel to units of Watts cm⁻² sr⁻¹ of known irradiance at the sensor.

Atmospheric corrections were done using a radiative transfer algorithm developed by NASA (Rickman et al., 2000; Schiller and Luvall, 2000). To accomplish this correction the software uses the relative positions of the target, sun, and aircraft for each pixel and adjusts the atmospheric correction accordingly. The algorithm used radiative transfer characteristics modeled with MODTRAN. Model inputs to MODTRAN included radiosonde data obtained via the National Climatic Data Center, sensor attributes and location specific variables such as altitude, orientation, visibility, and time. Post acquisition the flights were manually divided into straight line segments by visual inspection. Segments had <5° of departure from a straight line over total length. For each "straight path" flight segment MODTRAN estimates of transmittance and path radiance or single path scattering were generated. For each band, estimates are made at three different viewing

angles: before nadir, at-nadir, and after nadir. Regularity of radiative transfer characteristics as functions of angle then permitted estimates to be obtained for all other angles of interest. The MODTRAN values are then integrated over the sensor band passes. Thus unique atmospheric correction terms are available for each flight line segment as functions of angle from nadir. The calibrated value for each pixel was then integrated with the MODTRAN estimate of atmospheric transmissivity and "additive path radiance" as functions of angle from nadir. Energy at target can be calculated by rearranging and solving the basic equation:

$$E_s = E_t t + EA, \quad [1]$$

where E_s equals energy at sensor, E_t equals energy at target, t equals transmissivity, and EA equals "additive path radiance" which can be either true radiance and or scattered energy depending on wavelength. For a detailed description of the atmospheric algorithm and physics the reader is referred to Rickman et al. (2000) or Schiller and Luvall (2000).

Airborne Terrestrial Applications Sensor data were acquired for each site close to solar noon, under clear conditions on 2 June 2000 and 30 July 2001. Observations from the Coastal Plain site were limited to the 2000 data acquisition. Pixels lying completely within each plot were extracted, with each plot consisting of 16 pixels. Surface features and atmospheric attributes were assumed to be equal within each plot, thus the distribution of pixel values about mean plot values and percentage of coefficients of variation (CV) were used to assess sensor noise. Based on this analysis, during the 2000 acquisition <5% of the pixels sampled in most bands were greater than two standard deviations from mean plot values. However, in 2001, the percentage of pixels falling greater than two standard deviations from mean plot values was greater than in 2000. Coefficients of variation within plots were generally <10% in 2000, but as high as 36% in 2001. Furthermore, % CV showed that ATLAS bands 1 (450–520 nm) and 8 (2080–2350 nm) exhibited the most variability in 2000 and bands 1 to 3 within the 450- to 630-nm range were most variable in 2001. In 2001, ATLAS Bands 3 (600–630 nm) and 10 (8200–8600 nm) were faulty and excluded from analyses.

Statistical Analysis

Multivariate spectral data were first subject to band selection using a principal components analysis (PCA), since data encompassed multiple bands within the red, NIR, and TIR spectrum. Next, Duncan's least significant difference routine was used to delineate significant spectral differences ($\alpha = 0.10$) and determine the magnitude of spectral differences between treatments. Based on these results, stepwise linear regression analysis was used to determine the degree of variability in wheat straw residue that could be explained via remotely sensed data.

RESULTS AND DISCUSSION

Spectroradiometer Data

Spectral Response Curves

Spectral response curves (520–900 nm) were evaluated for each site and date. Spectral response patterns typical of living plant tissue were absent in residue. Instead, spectral response patterns of residue were similar to the soil spectral response line, with reflectance increasing without inflection throughout the VIS and NIR

Table 2. Specifications for the Airborne Terrestrial Applications Sensor (ATLAS) (2.5-m spatial resolution).

Wavelength	Band	Spectrum region
nm		
450–520	B1	visible-blue
520–600	B2	visible-green
600–630	B3	visible-red
630–690	B4	visible-red
690–760	B5	visible-red
760–900	B6	near infrared
1 550–1 750	B7	middle infrared
2 080–2 350	B8	middle infrared
8 200–8 600	B10	thermal infrared
8 600–9 000	B11	thermal infrared
9 000–9 400	B12	thermal infrared
9 600–10 200	B13	thermal infrared
10 200–11 200	B14	thermal infrared
11 200–12 200	B15	thermal infrared

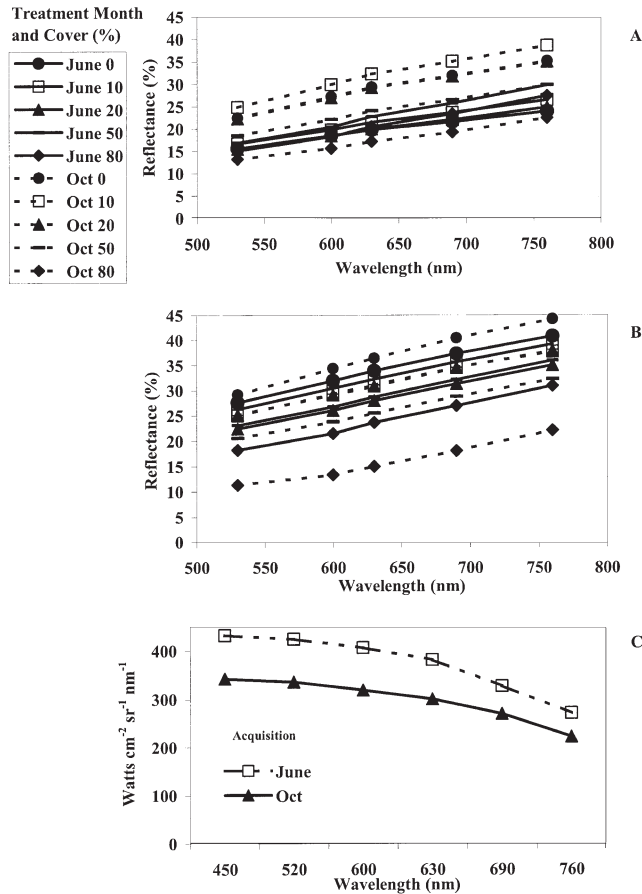


Fig. 1. Spectral response curves for each residue coverage as measured via a handheld spectroradiometer at the (A) Coastal Plain and (B) Appalachian Plateau study sites with corresponding total reflectance obtained via a spectralon reference plate at the (C) Appalachian Plateau for two periods in 2000.

(Fig. 1). Spectral response patterns were relatively consistent between sites and dates, but the magnitude of reflected energy varied. Conditions such as incoming radiant energy, water content, and residue decomposition at the time of RS data capture contributed to this variability. Analysis of total reflected energy from the spectralon reference plate provides evidence of differing atmospheric conditions, which were of a significant magnitude to elicit changes in the “at-sensor” reflectance properties. Data acquired in June and October 2000 for the Appalachian Plateau site exemplify differences in atmospheric conditions via a change in total reflected energy from the spectralon reference plate (Fig. 1). No differences in soil water content were observed between treatments during any one data acquisition; however, differences in average soil water content were observed between RS data acquisitions, particularly at the Appalachian Plateau site. Increasing soil water content tends to darken surfaces and reduce the amount of reflected energy, as a greater proportion of radiant energy is absorbed by the surface (Capehart and Carlson, 1997). This was observed in the 2000 Appalachian Plateau data set where average reflectance (600–630 nm) of bare soil plots ranged from 15 to 34% with peak reflectance during periods of low soil water content ($\theta_g < 2\%$) being more

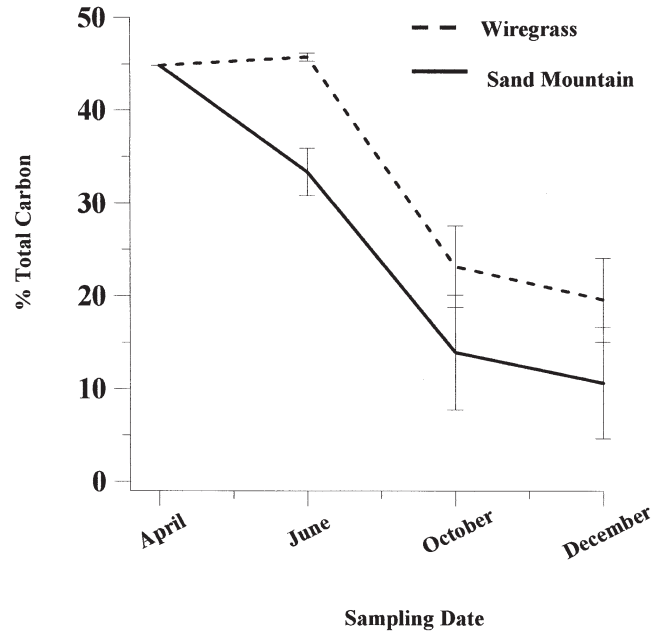


Fig. 2. Average C content of wheat straw at various sampling times in 2000 at the Coastal Plain and Appalachian Plateau study sites.

than twice that observed under wetter conditions ($\theta_g > 10\%$). Residue degradation also impacted spectral response patterns. Throughout the growing season, the total C content (TC) of residue gradually declined from 50 to $<25\%$ TC, suggesting decomposition of residue (Fig. 2). Residue cover differences were best observed during late-spring and fall, and related to decomposition of residue as treatment differences were best when residue TC $\leq 25\%$.

These data suggest that differences in the intensity of spectral response are critical to accurately depict the variability in residue coverage. Furthermore, differences in near-surface soil attributes impact the relative magnitude of spectral response. Soils in this study were dominated by sandy surfaces, predominately composed of quartz, and had similar spectra compared with fresh residue (Table 1); however, as residue degradation progressed, spectral differences between residue and soil became more evident.

Residue Coverage

Differentiation between residue treatments was best observed using a combination of bands in the 600- to 760-nm range (red–NIR). These results are consistent with previous studies, indicating red and NIR spectra best differentiate between residue cover differences (Biard and Baret, 1997; Nagler et al., 2000). Results showed that spectroradiometer data, at the spectral and spatial resolution used, could differentiate between plots receiving 20, 50, and 80% residue cover (Fig. 3). The relative magnitude of difference between bare soil plots and treatment plots varied during the collection period, with the greatest differences among treatments occurring during the October collection period, when TC content of the residue was $<25\%$.

Using a combination of red and NIR spectra in step-

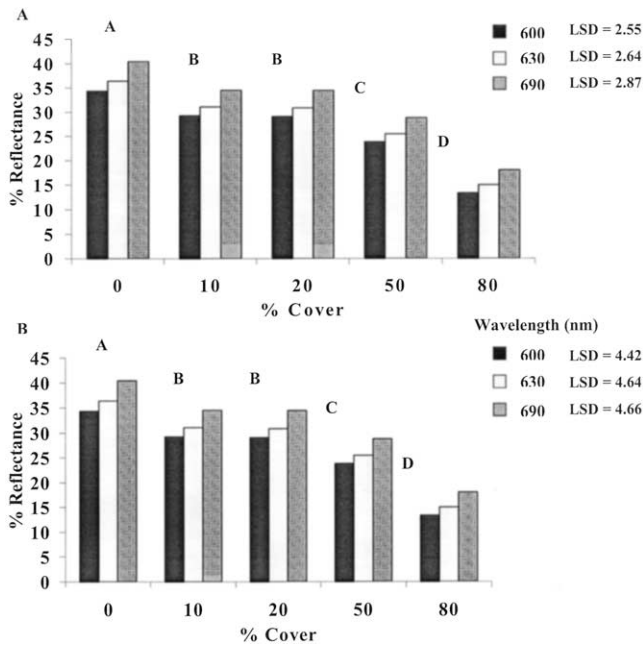


Fig. 3. Effects of wheat (*Triticum aestivum* L.) straw surface coverage on reflectance measured by a handheld spectroradiometer at the Appalachian Plateau in June and October of 2000.

wise regression improved our ability to depict differences in residue cover at each site. At the Coastal Plain location, a stepwise linear regression explained 69 to 82% of the variability in residue cover in 2000 and 65 to 72% of the variability in 2001 (Table 3). Spectroradiometer data acquired from the Appalachian Plateau study site accounted for 73 to 86 and 43 to 86% of the variability in 2000 and 2001, respectively (Table 3).

ATLAS Multispectral Scanner

Using all ATLAS bands, the first principal component explained 85% of the variance, with similar loading

factors for each band (ranging from 25 to 29%). Thus, analyses concentrated on bands that best differentiated between residue treatments, instead of bands that best described data variability. In most cases, reflectance within the 600- to 760-nm range and emittance in the 8200- to 9600-nm range best differentiated between treatments.

Spectral Response Curves

Visible and NIR spectral response patterns were similar to the bare soil line, differing only in magnitude of spectral response. Reflectance in the VIS portion of the spectrum slowly increases to a peak reflectance at approximately 760 nm, and then declines rapidly into the middle infrared regions (Fig. 4). Unlike VIS and NIR spectra, TIR spectral response curves differed in slope and magnitude of response when compared with the bare soil line. With <20% residue cover, soil spectral response dominated the shape of the spectral response curve with plots receiving residue distinguishable only by magnitude of spectral response (Fig. 4). However, as the amount of residue cover increased, the slope of the residue line for plots receiving 50 or 80% cover becomes positive in the 8200- to 8600-nm region and levels off in the 8600- to 9200-nm region. Beyond this point, emittance decreases rapidly and residue cover treatments are mostly indistinguishable.

Residue Coverage

During the 2000 data acquisition at the Appalachian Plateau site, reflected red energy in three different ATLAS bands successfully differentiated between plots receiving 10, 20, 50, and 80% cover (Fig. 5). Results from this study were based on atmospherically corrected ATLAS data, which facilitates the detection of differences between near surface attributes with similar spec-

Table 3. Stepwise linear regression parameters ($p < 0.10$) used to predict wheat (*Triticum aestivum* L.) straw cover based on percentage of reflectance from select spectroradiometer bands within the red and NIR regions for the Coastal Plain study site.

Date	Coastal Plain				Appalachian Plateau			
	Wavelength	Slope	Intercept	R^2	Wavelength	Slope	Intercept	R^2
Apr-00	630–690	–39.13		0.80	NS	NS	NS	NS
	690–760	34.21	38.10					
May-00	600–630	–27.96		0.82	NS	NS	NS	NS
	690–760	21.59	48.42					
Jun-00	NS†	NS	NS	NS	600–630	–34.41		
Oct-00	600–630	–48.41		0.69	690–760	28.22	47.42	0.80
	690–760	41.11	17.93		600–630	–0.34	115.51	0.86
Nov-00	600–630	–3.73	107.90	0.76	600–630	–70.65		
					630–690	60.53	90.68	0.73
Dec-00	600–630	–55.66		0.77	NS	NS	NS	NS
	630–690	51.54	30.56					
Apr-01	NS		NS	NS	NS	NS	NS	NS
May-01	600–630	–14.20		0.65	NS	NS	NS	NS
	690–760	14.86	–65.48					
Jun-01	NS	NS	NS	NS	600–630	–14.95		
Oct-01	600–630	–17.95		0.66	630–690	13.60	50.40	0.86
	690–760	15.61	53.58		600–630	–8.68		
Nov-01	600–630	–20.28		0.72	690–760	6.88	52.52	0.67
	690–760	15.88	71.43		600–630	–2.21	91.26	0.80
Dec-01	600–630	–33.65		0.72	600–630	–4.08	116.09	0.43
	690–760	28.06	33.78					

† NS indicates no significant regression relationship was observed.

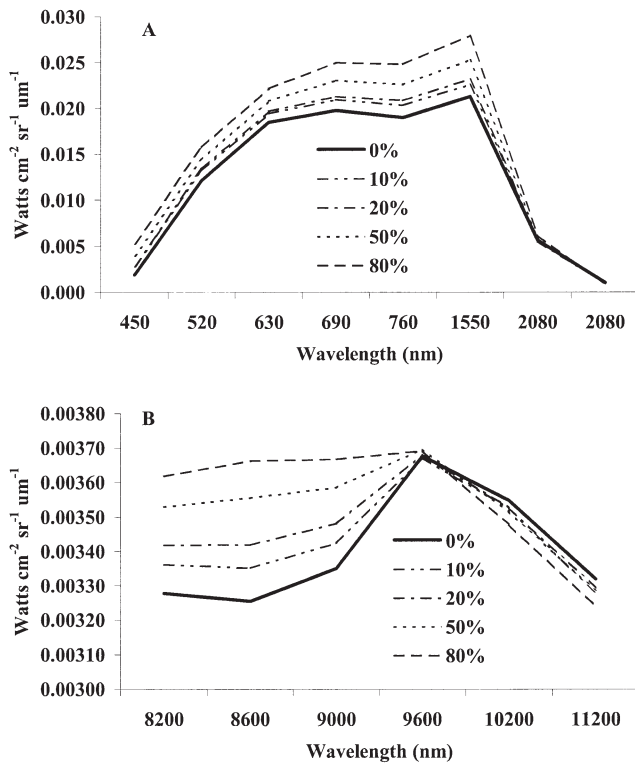


Fig. 4. Spectral response curves for each residue coverage as measured by the Airborne Terrestrial Applications Sensor (ATLAS) in the visible and near-infrared (A) and thermal infrared (B).

tral responses. In 2001, treatment differentiation of straw coverage was less clear and airborne RS data differentiated only between light (<20%) and heavy (>50%) cover treatments. A comparison of RS datasets acquired during a relatively dry year (2000) and a relatively wet year (2001) exemplify differences in spectral response associated with soil water content. In 2001, treatment separation was limited by higher soil water content ($\theta_g = 9.9\%$) compared with relatively drier ($\theta_g = 1.2\%$) surface conditions in 2000. Near-surface water absorbs a greater proportion of energy, thereby reducing the magnitude of difference in reflected energy for each treatment (Capehart and Carlson, 1997). At the Coastal Plain site, ATLAS Band 6 (red) best distinguished between 20, 50, and 80% cover, with no treatment differences between 0, 10, and 20% cover.

In 2000, TIR successfully differentiated between all cover treatments at both locations (Fig. 5). Results from the Appalachian Plateau site for 2001 showed TIR was only able to differentiate among 0, 20, and 80% cover treatments, possibly due to relatively higher soil water content at the time of data acquisition (data not shown). Our results demonstrate that lower heat capacities of organic materials, such as residue, resulted in greater emittance as residue coverage increased (Campbell, 1996). As a result, temperature differences between treatments associated with contrasting heat capacities of straw and bare soil likely facilitated in situ residue evaluation.

Regression analyses confirmed that a highly significant linear relationship ($P < 0.0001$) existed between emittance and residue cover at the Appalachian Plateau

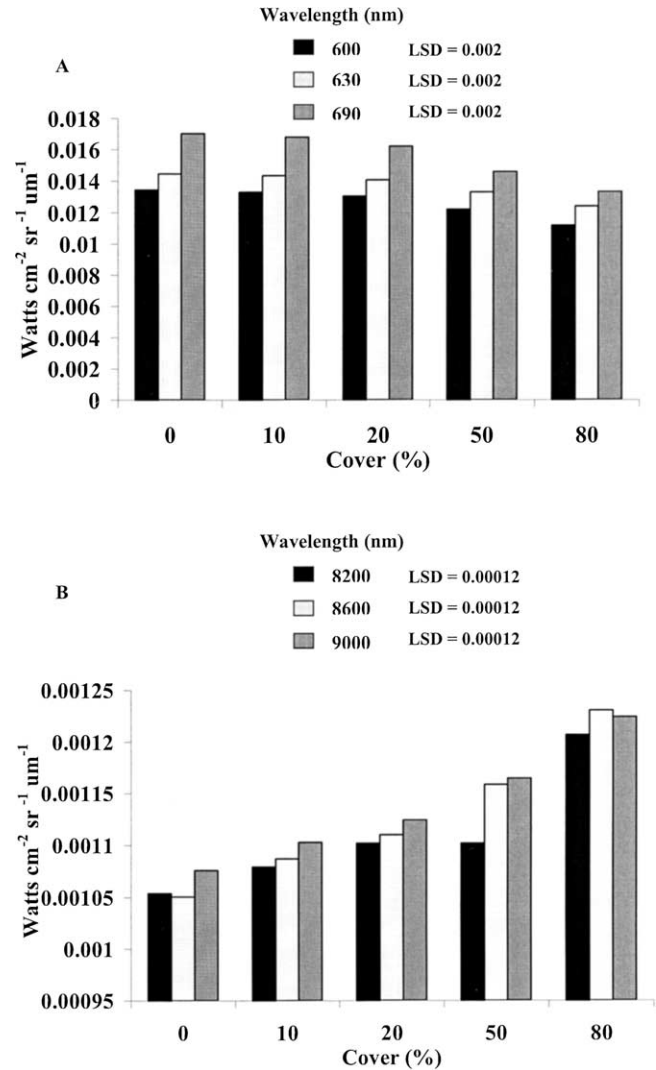


Fig. 5. Effects of wheat (*Triticum aestivum* L.) straw surface coverage on spectral response measured by the Airborne Terrestrial Applications Sensor (ATLAS) at the Appalachian Plateau site during the June 2000 data acquisition.

site. Thermal infrared spectra resulted in r^2 peaking at 0.98 and 0.83 in 2000 and 2001, respectively (Table 4). Visible-red spectra were also useful, accounting for as much as 98% of the residue variability in 2000 and 74% of the residue variability in 2001. Under relatively dry conditions in 2000, TIR data explained 95% of the residue variability at the Coastal Plain site while, VIS-red spectra accounted for 77–81% of the variability in residue cover (Table 4).

CONCLUSION

Results demonstrate the utility and potential limitations associated with using handheld or airborne RS data to depict differences in residue coverage. Typical residue spectral response curves in the VIS and NIR regions of the spectrum differed from bare soil spectra mostly in magnitude of spectral response. Residue cover separation was partially a function of straw decomposition, and soil water content at the time of acquisition. As resi-

Table 4. Regression parameters ($p < 0.10$) relating wheat (*Triticum aestivum* L.) straw cover (0, 10, 20, 50, and 80%) to reflected or emitted energy ($\text{Watts cm}^{-2} \text{sr}^{-1} \mu\text{m}^{-1}$) acquired via the Airborne Terrestrial Applications Sensor (ATLAS). Data were acquired for the Coastal Plain (2000) and Appalachian Plateau study sites (2000 and 2001).

Year	Coastal Plain				Appalachian Plateau			
	Wavelength	Slope	Intercept	R^2	Wavelength	Slope	Intercept	R^2
	nm				nm			
2000	600–630	37 651	–225.03	0.71	600–630	–31 153	422.23	0.98
	630–690	28 510	–181.85	0.77	630–690	–33 898	493.45	0.98
	690–760	26 398	–162.06	0.79	690–760	–18 384	315.32	0.97
	8 200–8 600	535 514	–586.98	0.95	8 200–8 600	503 046	–534.17	0.98
	8 600–9 000	444 929	–484.15	0.95	8 600–9 000	437 690	–465.69	0.97
2001	9 000–9 400	574 441	–643.36	0.95	9 000–9 400	525 612	–570.53	0.97
					600–630	NS	NS	NS
					630–690	–9 092.00	106.97	0.70
					690–760	–11 001	133.52	0.74
					8 200–8 600	NS	NS	NS

due degradation progressed, however, NIR spectra could be used to differentiate among plots receiving greater than 20% residue coverage.

Comparison of ATLAS imagery to handheld spectroradiometer data demonstrate the role atmospherically corrected, high spectral resolution, airborne imagery can play in rapid assessment of residue cover. First, VIS and NIR ATLAS datasets more clearly differentiated among treatments compared with handheld spectroradiometer data. Second, ATLAS results showed that high spectral resolution TIR imagery more accurately delineated treatment differences compared with VIS and NIR spectra. Emitted energy is a function of the emissivity of an object and its temperature; hence emittance is intrinsic to the object of interest, whereas reflected energy is an indirect measure of the state of a given ground feature. Thus, plots receiving greater amounts of residue cover are distinguishable based on the differing heat capacities of organic (residue) and mineral (soil) surfaces. All other conditions being equal, our data suggest TIR is a more stable assessment residue cover compared with VIS and NIR. Another benefit of airborne imagery is a function of spatial representation. ATLAS data captured “whole-plots” compared with handheld datasets that consisted of a limited number of samples within each plot. Thus, the ATLAS sensor likely captured a more representative sample of the variability in residue distribution within the plot.

Overall, residue cover and spectral response exhibited a significant ($p \leq 0.05$) linear relationship. Data acquired using ATLAS provided the most accurate results throughout the VIS, NIR, and TIR ($r^2 = 0.77$ – 0.98). Results were best when surfaces were dry ($\theta_g < 2\%$). Monthly spectroradiometer data were useful in estimating residue cover by combining two bands in the red and NIR region using linear regression ($r^2 = 0.65$ – 0.86).

REFERENCES

- Aase, J.K., and D.L. Tanaka. 1991. Reflectances from four wheat residue cover densities as influenced by three soil backgrounds. *Agron. J.* 83:753–757.
- Biard, F., and F. Baret. 1997. Crop residue estimation using multiband reflectance. *Remote Sensing Environ.* 59:530–536.
- Birk, J.B. 1992. Commercial applications multispectral sensor system. *Small Satellite Technologies and Applications II*. 1691:49–59.
- Capehart, W.J., and T.N. Carlson. 1997. Decoupling of surface and near-surface soil water content: A remote sensing perspective. *Water Resour. Res.* 33:1383–1395.
- Campbell, J.B. 1996. *Introduction to remote sensing*. 2nd ed. The Guilford Press, New York.
- Daughtry, C.S.T., J.M. McMurtrey, III, E.W. Chappelle, W.P. Dulaney, J.R. Irons and M.B. Satterwhite. 1995. Potential discriminating crop residues from soil by reflectance and fluorescence. *Agron. J.* 87:165–171.
- Daughtry, C.S.T., P.L. Nagler, M.S. Kim, J.E. McMurtery, III, and E.W. Chappelle. 1996. Spectral reflectance of soils and crop residues. p. 505–510. *In* A.M.C. Davies and P. Williams (ed.) *Near infrared spectroscopy. The future waves*. NIR Pub., Chichester, UK.
- Daughtry, C.S.T. 2001. Discriminating crop residues from soil by short-wave infrared reflectance. *Agron. J.* 93:125–131.
- Elvidge, C.D. 1990. Visible and near-infrared reflectance characteristics of dry plant materials. *Int. J. Remote Sensing*. 10:1775–1795.
- Gausman, H.W., and W.A. Allen. 1973. Optical properties of leaves of 30 plant species. *Plant Physiol.* 52:57–62.
- Jackson, M.L. 1975. *Soil chemical analysis—Advanced course*. Published by the author, M.L. Jackson, Madison, WI.
- Kilmer, V.J., and L.T. Alexander. 1949. Methods of making mechanical analysis of soils. *Soil Sci.* 64:1–24.
- Lal, R., and J.M. Kimble. 1997. Conservation tillage for carbon sequestration. *Nutr. Cycling Agroecosyst.* 49:243–253.
- McMurtrey, J.E., III, E.W. Chappelle, C.S.T. Daughtry, and M.S. Kim. 1993. Fluorescence and reflectance of crop residue and soil. *J. Soil Water Conserv.* 48:207–213.
- Murray, I., and P.C. Williams. 1988. Chemical principles of near infrared technology. p. 17–34. *In* P. Williams and P. Norris (ed.) *Near-infrared technologies in the agricultural and food industries*. Am. Assoc. Cereal Chemists, St. Paul, MN.
- Prasad, R., and J.F. Power. 1991. Crop residue management-literature review. *Adv. Soil Sci.* 15:205–251.
- Nagler, P.L., C.S.T. Daughtry, and S.N. Goward. 2000. Plant litter and soil reflectance. *Remote Sens. Environ.* 71:207–215.
- Rickman, D.L., S. Schiller, and J. Luvall. 2000. Physics for the correction of a calibrated airborne scanner, visible to thermal bands. *Workshop on Multi/hyperspectral Sensors, Measurements, Modeling and Simulation*, U.S. Army Aviation & Missile Command, Redstone Arsenal, AL, 7–9 Nov. 2000.
- Schiller, S., and J. Luvall. 2000. Description and performance demonstration of the portable ground-based atmospheric monitoring system (PGAMS) for optimal radiative transfer modeling, atmospheric correction and vicarious sensor calibration, modeling and simulation. *U.S. Army Aviation & Missile Command, Redstone Arsenal, AL, 7–9 Nov. 2000.*
- USDA. 1995. *Crop residue management to reduce erosion and improve soil quality*. Conservation Research Rep. 39. U.S. Gov. Print. Office, Washington, DC.